# New coherence effects in the polarization of light emitted by photofragments: Theory

M. Glass-Maujean
*Laboratoire de Spectroscopie Hertzienne de l'Ecole Normale Supérieure, Université Pierre et Marie Curie, 75252 Paris, Cedex 05, France*

J. Alberto Beswick
*Laboratoire pour l'Utilisation du Rayonnement Electromagnétique, Université de Paris-Sud, 91405 Orsay, France*
(Received 3 March 1987)

A quantum-mechanical treatment of the degree of polarization of photofragment fluorescence in the case where two dissociative electronic states of different symmetry with the same limit are excited coherently is presented. This results in an interference effect which depends both on the photoabsorption probability amplitudes in the different excited states as well as on the phase differences of their vibrational wave functions at large distances. Oscillations of the polarization ratio as a function of the photon energy are predicted. Applications to some simple cases involving a diatomic molecule initially in a $^1\Sigma$ state are presented. The case of $Ca_2$ is discussed. The role of fine (or hyperfine) structure, and in particular the case of unresolved fluorescence is treated. The classical model in terms of oscillating electric dipole moments properly averaged over the initial orientations of the molecule is presented and allows the interpretation of the quantum results.

## I. INTRODUCTION

Following the van Brunt and Zare pioneering theoretical paper[1] on polarization of the light emitted by photofragments, a wealth of experimental and theoretical work in this area has been performed.[2–12]

Consider, for instance, a diatomic molecule $AB$ in a ground $^1\Sigma$ state excited to a dissociative $^1\Pi$ continuum leading to $A^*(^1P)+B(^1S)$ atomic fragments. Since $\Lambda=\pm1$ for a $\Pi$ state, the excited atomic fragment $A^*(^1P)$ can only be populated in the magnetic sublevels $m_L=\pm1$, the internuclear vector being the quantization axis. For an incident linearly polarized light, photodissociation not only produces alignment of the fragments but also populates the atomic $m_L=\pm1$ magnetic sublevels in a coherent superposition.[8,9] This results in a degree of polarization

$$P=\frac{I_{\parallel}-I_{\perp}}{I_{\parallel}+I_{\perp}} \tag{1}$$

(where $I_{\parallel}$ and $I_{\perp}$ refer to the incident polarization direction), which is very different from the value obtained ignoring the induced coherence.[1]

In this paper we shall show that other coherences may be produced in the populations of the magnetic sublevels with different $|m_L|$ values. Consider, for example, the case discussed above, namely a $A^*(^1P)+B(^1S)$ dissociation limit. Two molecular singlet states $^1\Pi$ and $^1\Sigma$ are correlated to this limit. They can both be reached by optical excitation from a $^1\Sigma$ ground state and their excitation should necessarily be coherent. Since the $^1\Pi$ state produces only $m_L=\pm1$ levels of the $A^*(^1P)$ fragments (in a coherent superposition, of course), and the $^1\Sigma$ state produces $A^*(^1P)$ fragments with $m_L=0$, there will be an additional coherence between the $m_L=0$ and the $m_L=\pm1$ magnetic sublevels. We therefore expect a change on the polarization degree of the fragment fluorescence due to such coherent excitation. This effect will be particular important if the photoabsorption cross sections for the $\Pi$ and $\Sigma$ states are of comparable strength. We shall also show that it depends on the asymptotic relative phases of the continuum final vibrational wave functions. Since both the excitation amplitudes and phases depend on the excess energy, we predict a dependence of the polarization degree with the photon energy.

There is another issue concerning the degree of polarization of photofragments which is addressed in this paper, namely the effect of unresolved fine (or hyperfine) structure. In a recent paper,[10] Singer, Freed, and Band have calculated the degree of polarization for fluorescence from atomic fragments produced in excited fine-structure states for a variety of systems. In their treatment it is assumed that the fluorescence from individual fine-structure levels can be detected. We present here the case of unresolved fine- or hyperfine-structure emission and we show that the polarization degree is modified.

This paper will be organized as follows. In Sec. II we present the general quantum-mechanical formalism in the axial-recoil approximation together with a classical picture in terms of oscillating electric dipole moments. We consider the case where the fluorescence lifetime is much longer than the dissociation lifetime so that effects due to short times emission following photodissociation are negligible. In Sec. III the results for some simple cases involving a diatomic molecule initially in a $^1\Sigma$ state are given. In Sec. IV we discuss these results and we provide their classical interpretation. Finally Sec. V is devoted to the conclusions.

 

## II. QUANTUM-MECHANICAL TREATMENT OF THE POLARIZATION OF THE FRAGMENT FLUORESCENCE

### A. General formulation

Polarization of the light emitted by photodissociation fragments was first considered by van Brunt and Zare.[1] In their treatment the atomic fragment is assumed to be formed by photodissociation in an incoherent superposition of the magnetic sublevels. The calculation is then performed in two steps: (i) evaluating the parallel and perpendicular polarization intensities for each possible orientation of the internuclear axis in space and (ii) averaging the intensities over the angular distribution of the internuclear axis after photodissociation (the fluorescence is assumed to be much slower than dissociation, so that the photon is emitted well after the dissociation is completed).

Vigué *et al.*[8] have shown that in many cases the atomic fragments are formed in a coherent superposition of the magnetic sublevels. The result is a polarization degree which can be very different from the one obtained with the assumption of incoherent superposition. For instance, the latter will give (in the axial-recoil limit, i.e., when dissociation proceeds fast as compared with the rotational period of the molecule)

$$P=(3\langle\cos^2\gamma\rangle-1)/(\langle\cos^2\gamma\rangle+3)\ , \tag{2}$$

where $\gamma$ is the angle between the absorbing and emitting transition dipole moments in the molecular frame and $\langle\ \rangle$ denotes the average over all possible initial orientations of the molecule. This result is well known in the theory of luminescence and can be obtained by a simple semiclassical model in terms of absorbing and emitting linear oscillators.[13] According to (2) the degree of polarization should be between $-\frac{1}{3}$ and $+\frac{1}{2}$.

On the other hand, when $m_L=\pm1$ coherence effects are included, Vigué *et al.*[8] have calculated a maximum of $P=0.78$ for a $^1\Pi$ state dissociating into a $^1P$ excited atom. A general quantum-mechanical treatment to deal with those problems has been presented.[9] The photon excitation, dissociation, and fluorescence decay were treated together both for a direct-photodissociation process as well as for predissociation. We shall follow here the same general treatment. We thus describe the molecular system by three sets of eigenstates: $|A_i\rangle$ for the initial state, $|A_f\rangle$ for the final state after photon decay, and $|A_d\rangle$ for the excited dissociative state. The process we are interested in corresponds to the excitation of the $|A_d\rangle$ state by photon absorption (with wave vector $\mathbf{k}_i$ and polarization $\mathbf{e}_i$), from an initial state $|A_i\rangle$ and then decay by photon emission (with wave vector $\mathbf{k}_f$ and polarization $\mathbf{e}_f$):

$$|A_i\rangle \xrightarrow{\mathbf{k}_i,\mathbf{e}_i} |A_d\rangle \xrightarrow{\mathbf{k}_f,\mathbf{e}_f} |A_f\rangle\ . \tag{3}$$

The partial-differential cross section for this process is given by[9] (in esu)

$$\frac{d\sigma}{d\hat{\Omega}_f}=\sum_{A_f}k_f^3k_i\left|\sum_{A_d}\frac{\langle A_i|\mathbf{D}\cdot\mathbf{e}_i|A_d\rangle\langle A_d|\mathbf{D}\cdot\mathbf{e}_f^*|A_f\rangle}{E-E_d+i\Gamma_d}\right|^2, \tag{4}$$

where $E_d$ is the energy of the dissociative state, while $\Gamma_d$ is the radiative linewidth of the emitting state. In Eq. (4), $E$ is the total energy $E=E_i+\hbar k_i c$. Each one of the wave functions can be decomposed [in Hund's case (a)] as

$$|A\rangle=\Phi_A(r,R)\frac{\chi_A(R)}{R}|\alpha\rangle\ , \tag{5}$$

where $\Phi_A$ is the electronic part, $\chi_A$ is the vibrational wavefunction, while $|\alpha\rangle$ is the rotational and spin angular momentum part. Similarly, the dipole operator $\mathbf{D}$ can be decomposed in radial and angular parts. We shall write

$$\mathbf{D}\cdot\mathbf{e}_i=er\left[\frac{\mathbf{r}}{r}\cdot\mathbf{e}_i\right]=erD_i\ . \tag{6}$$

We then have for the matrix elements in (2)

$$\langle A_i|\mathbf{D}\cdot\mathbf{e}_i|A_d\rangle=\int dR\,\chi_i(R)\chi_d(R)\times\int dr\,r^3\Phi_i(r,R)\Phi_d(r,R)\times\langle\alpha_i|D_i|\alpha_d\rangle\ , \tag{7a}$$

$$\langle A_d|\mathbf{D}\cdot\mathbf{e}_f|A_f\rangle=\int dR\,\chi_d(R)\chi_f(R)\times\int dr\,r^3\Phi_d(r,R)\Phi_f(r,R)\times\langle\alpha_d|D_f^*|\alpha_f\rangle\ . \tag{7b}$$

### B. Direct dissociation

Equation (7b) can be simplified in the case of direct dissociation where fragmentation is fast compared to the radiative lifetime.[9] This amounts to considering the situation where emission occurring during dissociation is negligible. This is opposite to the case corresponding to ringing effects.[14–17] In this case, the main contribution to (7b) comes from the asymptotic region (the emission occurs at large $R$) and the electronic integral can be replaced by its atomic value $\mathcal{R}_f$. We then have

$$\langle A_d|\mathbf{D}\cdot\mathbf{e}_f^*|A_f\rangle=\mathcal{R}_f\langle\chi_d|\chi_f\rangle_R\langle\alpha_d|D_f^*|\alpha_f\rangle\ . \tag{8}$$

The sum over all the intermediate states $A_d$ in Eq. (4) implies a sum over all electronic states accessible, a sum over the rotational states as well as the integral over the kinetic energy $\varepsilon_d$ since the intermediate states are dissociative. Let us consider the integral over $\varepsilon_d$ first.

Using (8) and the asymptotic form of the continuum vibrational wave functions

$$|\chi\rangle\underset{R\to\infty}{\cong}(2\mu/\pi\hbar^2)^{1/2}[\sin(kR+\varphi)/k^{1/2}]\ , \tag{9}$$

where $k=(2\mu\varepsilon_d)^{1/2}/\hbar$, one obtains[9]

$$\int_0^\infty d\varepsilon_d \frac{\langle A_i \mid \mathbf{D}\cdot\mathbf{e}_i \mid A_d\rangle\langle A_d \mid \mathbf{D}\cdot\mathbf{e}_f^* \mid A_f\rangle}{E-E_d+i\Gamma_d} \simeq \mathcal{R}_f\langle\alpha_i \mid D_i \mid \alpha_d\rangle\langle\alpha_d \mid D_f^* \mid \alpha_f\rangle \frac{\langle\chi_i \mid \mathcal{R}_{\rm mol} \mid \chi_d\rangle e^{i(\varphi_f-\varphi_i)}}{E-(\varepsilon_f+E_d^{(\rm at)})+i\Gamma_d} , \tag{10}$$

where $E_d^{(\rm at)}$ is the internal energy of the excited atomic fragments. We have also denoted by $\mathcal{R}_{\rm mol}$ the radial part of the molecular-transition dipole moment

$$\int dr\, r^3 \Phi_i(r,R)\Phi_d(r,R) .$$

We now turn to the sum over the final states $A_f$ in Eq. (4), which implies an integral over the relative kinetic energy $\varepsilon_f$. Introducing Eq. (10) into Eq. (4), we shall have integrals of the form

$$\int d\varepsilon_f \frac{1}{[E-(\varepsilon_f+E_d^{(\rm at)})+i\Gamma_d][E-(\varepsilon_f+E_{d'}^{(\rm at)})-i\Gamma_{d'}]} . \tag{11}$$

We need now to specify the electronic states $d$ of the excited atomic fragments. Except for the very particular case of electronic and nuclear spin equal to zero, the atomic states is a multiplet (fine or hyperfine structure). We then have a sum over $d$ and $d'$ of Eq. (11) with squared ($d=d'$) and cross ($d\neq d'$) terms. For $d=d'$, the integral (11) gives the result obtained in Ref. 9, i.e., $\pi/\Gamma_d$ with $\Gamma_d$ being the radiative linewidth of the atomic fragment emitting state $\Gamma^{(\rm at)}$ which is the same for all the components of the multiplet.[18]

On the other hand, for $d\neq d'$ and the kinetic energy larger than the multiplet splitting $\Delta E=E_d-E_{d'}$, one obtains:

$$\frac{\pi(\Gamma^{(\rm at)}+i\Delta E/2)}{(\Delta E/2)^2+(\Gamma^{(\rm at)})^2} . \tag{12}$$

Now in most cases the splitting $\Delta E$ is much larger than the radiative linewidth and therefore the cross terms can be neglected. In other words, the spin recoupling occurs in a time scale much shorter than photon emission and much longer than dissociation.[19]

Under these conditions, the differential partial cross section Eq. (4) reduces to

$$\frac{d\sigma}{d\hat{\Omega}_f} = \pi k_f^3 k_i e^4 \frac{R_f^2}{\Gamma^{(\rm at)}} \sum_f \sum_{d,d'} \langle\alpha_i \mid D_i \mid \alpha_d\rangle\langle\alpha_d \mid D_f^* \mid \alpha_f\rangle\langle\chi_i \mid \mathcal{R}_{\rm mol} \mid \chi_d\rangle\langle\chi_{d'} \mid \mathcal{R}_{\rm mol} \mid \chi_i\rangle\langle\alpha_f \mid D_f \mid \alpha_{d'}\rangle \times\langle\alpha_{d'} \mid D_i^* \mid \alpha_i\rangle\delta_{j_d j_{d'}} e^{i(\varphi_{d'}-\varphi_d)} , \tag{13}$$

where $j_d, j_{d'}$ are the angular momentum quantum numbers characterizing the multiplets.

Using the density-matrix formalism[20]

$$\frac{d\sigma}{d\hat{\Omega}_f} = 4\pi^2 k_i \sum_{\alpha_d\alpha_{d'}} \rho_{\alpha_{d'},\alpha_d}\mathcal{D}_{\alpha_d,\alpha_{d'}} e^{i(\varphi_{d'}-\varphi_d)}\delta_{j_{d'}j_d} , \tag{14}$$

where

$$\rho_{\alpha_{d'},\alpha_d} = e^2\langle\alpha_{d'} \mid D_i^\dagger \mid \alpha_i\rangle\langle\alpha_i \mid D_i \mid \alpha_d\rangle \times\langle\chi_{d'} \mid \mathcal{R}_{\rm mol} \mid \chi_i\rangle\langle\chi_i \mid \mathcal{R}_{\rm mol} \mid \chi_d\rangle \tag{15}$$

is the excitation matrix and

$$\mathcal{D}_{\alpha_d,\alpha_{d'}} = \frac{k_f^3\mathcal{R}_f^2 e^2}{4\pi\Gamma^{(\rm at)}}\langle\alpha_d \mid D_f^* \mid \alpha_f\rangle\langle\alpha_f \mid (D_f^*)^\dagger \mid \alpha_{d'}\rangle \tag{16}$$

is the detection matrix. The numerical factor introduced in $\mathcal{D}_{\alpha_d,\alpha_{d'}}$ is a normalization factor such that integration over all possible transitions, directions, and polarizations of the emitted photon gives 1.

In Eq. (14) the product

$$\tilde{\rho}_{\alpha_{d'},\alpha_d} = \rho_{\alpha_{d'},\alpha_d} e^{i(\varphi_{d'}-\varphi_d)}\delta_{j_{d'}j_d} \tag{17}$$

can be interpreted as the fragment-excitation matrix obtained by evolution during the dissociation (the phase-shift term) and the spin coupling (the $\delta_{j_{d'}j_d}$ term) of the molecular-excitation matrix $\rho_{\alpha_{d'},\alpha_d}$. Using Eq. (17), Eq. (14) reduces to the usual form[21]

$$\frac{d\sigma}{d\hat{\Omega}_f} = 4\pi^2 k_i \,\mathrm{Tr}(\tilde{\rho}\,\mathcal{D}) . \tag{18}$$

### C. Excitation of the molecule

#### 1. *Expressions of the excitation matrix $\rho$ for a $\Sigma$ initial state*

The laboratory $Z$ axis is chosen parallel to the incident polarization vector $\mathbf{e}_i$. For parallel $\Sigma\rightarrow\Sigma$ and perpendicular $\Sigma\rightarrow\Pi$ transitions, for example, the matrix elements $\rho_{\Lambda',\Lambda}$ can be easily calculated using Wigner-Eckart theorem with the result:

$$\rho_{1,1} = \tfrac{1}{2}(\sin^2\theta)M_\Pi^2 = \rho_{-1,-1} , \tag{19a}$$

$$\rho_{1,-1} = \rho_{-1,1} = -\rho_{1,1} , \tag{19b}$$

$$\rho_{0,0} = (\cos^2\theta)M_\Sigma^2 , \tag{19c}$$

$$\rho_{0,1} = -\frac{1}{\sqrt{2}}(\sin\theta)(\cos\theta)M_\Sigma M_\Pi = -\rho_{0,-1} = -\rho_{-1,0} = \rho_{1,0} , \tag{19d}$$

where the $M_\Lambda$ are the transition dipole-moment matrix elements

$$M_\Lambda = \langle\chi_\Sigma^{(i)} \mid \mathcal{M}_\Lambda \mid \chi_\Lambda\rangle , \tag{20}$$

with $\mathcal{M}_\Lambda$ being the electronic transition dipole moments

taking into account both the radial ($\mathcal{R}_{\rm mol}$) as well as the angular momentum part.[21] Actually the angular dependence of $\rho_{1,1}$ and $\rho_{0,0}$ corresponds to the usual anisotropy for absorption in the case of parallel and perpendicular transitions.[22] The angle $\theta$ is the polar angle specifying the direction of the internuclear axes with respect to the laboratory $Z$ axis (see Fig. 1).

The matrix elements $\rho_{1,-1}$ and $\rho_{-1,1}$ are responsible for the "coherence effect" calculated by Vigué *et al.*[8,9] The coherence elements $\rho_{0,1}$, $\rho_{1,0}$, $\rho_{0,-1}$, and $\rho_{-1,0}$, on the other hand, are responsible for interference between dissociations through electronic states with different symmetry ($\Sigma$ and $\Pi$ dissociative states). The study of the effect induced by such coherence matrix elements on the degree of polarization of photofragment fluorescence constitutes the major aim of this paper. It is important to note at this point that the coherences may exist here only because the $\Sigma$ and $\Pi$ levels are degenerate in the dissociation continua. Thus they can be excited by the same photon.

### 2. Physical interpretation

The physical interpretation of the excitation process can be easily provided by a classical transition dipole-moment vector $\mathbf{M}$ defined by

$$\mathbf{M}=\langle \Psi_i \mid \underline{\mathbf{M}} \mid \Psi_d \rangle \ , \tag{21}$$

where $\mid \Psi_i \rangle$ is the ground-state initial wave function, $\mid \Psi_d \rangle$ is the wave function of the excited state produced by the photon absorption, and $\underline{\mathbf{M}}$ is the transition dipole-operator vector with modulus equal to the transition amplitude $(M_\Sigma^2 \cos^2\theta + M_\Pi^2 \sin^2\theta)^{1/2}$ and directed along the electronic position vector $\hat{\mathbf{r}}$. In our case of linearly polarized light in the $Z$ direction, $\mid \Psi_d \rangle$ is given by[8]

$$\mid \Psi_d \rangle = \frac{(\cos\theta) M_\Sigma \mid \Sigma \rangle - \frac{1}{\sqrt{2}} (\sin\theta) M_\Pi ( \mid \Pi, \Lambda=+1 \rangle - \mid \Pi, \Lambda=-1 \rangle )}{[(\cos^2\theta) M_\Sigma^2 + (\sin^2\theta) M_\Pi^2]^{1/2}} \ . \tag{22}$$

Notice that this wave function is equivalent to the excitation matrix $\rho$ defined in Eq. (19).

Introducing Eq. (22) into Eq. (21) we obtain

$$\mathbf{M}=(\cos\theta) M_\Sigma \hat{\mathbf{z}} + (\sin\theta) M_\Pi \hat{\mathbf{x}} \ . \tag{23}$$

We notice that $\mathbf{M}$ lies on the plane defined by $\hat{\mathbf{Z}}$ and $\hat{\mathbf{z}}$ (see Fig. 2) as demonstrated by Vigué *et al.*[9] and which is a consequence of the axial symmetry of the molecule. The limiting cases $M_\Sigma=0$ or $M_\Pi=0$ give the expected results $[(\cos\theta) M_\Sigma \hat{\mathbf{z}}$ and $(\sin\theta) M_\Pi \hat{\mathbf{x}}$, respectively] for parallel and perpendicular transitions. For $M_\Sigma=M_\Pi$, one gets $\mathbf{M}$ parallel to $(\cos\theta)\hat{\mathbf{z}}+(\sin\theta)\hat{\mathbf{x}}=\hat{\mathbf{Z}}$, i.e., the result for an isotropic system (an atom, for instance).

## D. Evolution of the system while dissociating

### 1. Axial-recoil approximation

In the axial-recoil approximation it is assumed that dissociation occurs in a time scale much faster than the rotation of the molecular internuclear axis. Thus the direction of the internuclear axis remains the same during the whole process: absorption of a photon, dissociation, emission of fluorescence. This implies that the rotation of the molecular axis is not coupled to the electronic angular momentum.

Quantum mechanically, Eq. (14) gives the differential cross section for the process from an initial molecular state $\mid J_i, M_i \rangle$, where $J_i$ is the total angular momentum and $M_i$ its space-fixed component. If the molecule is initially randomly oriented one has to sum over $M_i$ Eq. (14). In addition, the sums over $\alpha_d$, $\alpha_{d'}$, and $\alpha_f$ imply sums over $J_d$, $M_d$, $J_{d'}$, $M_{d'}$, $J_f$, and $M_f$. In the limit of axial recoil,[22] the matrix elements $\langle \alpha_i \mid D_i \mid \alpha_d \rangle$, $\langle \alpha_d \mid D_f^* \mid \alpha_f \rangle$, etc., as well as the phases $\varphi_d$ are independent of the total angular momentum $J_d$. Under these conditions the above-mentioned summation can be carried out with the result that they no longer depend on the initial total angular momentum $J_i$. This is equivalent to

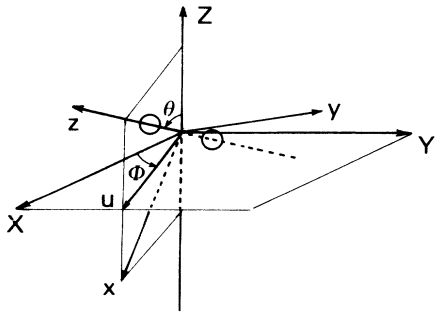


FIG. 1. Molecular ($xyz$) and laboratory ($XYZ$) reference systems. The incident polarization vector is along $Z$ while the diatomic internuclear axis is along $z$. $\theta$ and $\Phi$ are the polar angles specifying the orientation of the molecule.

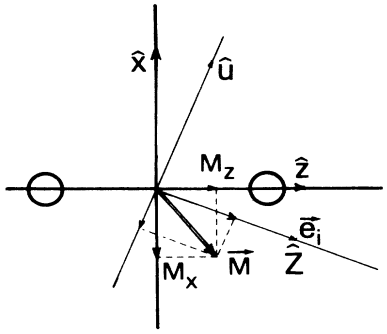


FIG. 2. Classical oscillating dipole $\mathbf{M}$ induced by the photon excitation. The dipole is in the plane $\hat{\mathbf{z}}\hat{\mathbf{Z}}$ defined by the internuclear axis and the incident polarization vector.

stating that the overall rotation of the molecule is neglected in this approximation. Therefore, the calculations can be conducted for fixed molecular orientations specified by polar angles $\theta$ and $\Phi$.

#### 2. Anisotropy of the photofragments angular distribution

In the axial-recoil approximation, the angular distribution of the photoejected fragments is given by the probability of exciting the molecule with a given orientation of the internuclear axis with respect to the laboratory frame

$$\sigma(\theta)=\pi k_i \,\mathrm{Tr}(\tilde{\rho})=\pi k_i \,\mathrm{Tr}(\rho) \,, \tag{24}$$

which using Eqs. (17) and (19) gives the expected angular distribution

$$\sigma(\theta)=\pi k_i (M_\Pi^2 \sin^2\theta + M_\Sigma^2 \cos^2\theta) \,. \tag{25}$$

We notice from Eq. (25) that $\sigma(\theta)$ is sensitive only to the population terms of the density-matrix $\rho$ and ignores all coherence terms $\rho_{10}$, $\rho_{1-1}$, etc. Equation (25) can now be written in the usual form

$$\sigma(\theta)=\sigma_0[1+\beta P_2(\cos\theta)] \,, \tag{26}$$

with

$$\beta=2\frac{M_\Sigma^2-M_\Pi^2}{M_\Sigma^2+2M_\Pi^2} \tag{27}$$

giving the well-known limits $\beta=2$ for $\Sigma\rightarrow\Sigma$ transition, $\beta=-1$ for a $\Sigma\rightarrow\Pi$ transition. It is interesting to note that in the very particular case $|M_\Pi|=|M_\Sigma|$, $\beta=0$, and the angular distribution is isotropic.

#### 3. Evolution

The effect of the evolution of the system during dissociation is expressed in Eq. (19) by the transition from the molecular-excitation matrix $\rho$ to the fragment-excitation matrix $\tilde{\rho}$ through the dephasing between different dissociative channels as well as the spin coupling at very large interfragment distance.

Coming back to the classical picture of the oscillating dipole given in Sec. II C 2, the dephasing between the dissociative channels corresponds to a dephasing between the $M_z$ and $M_x$ oscillating components

$$\mathbf{M}e^{i\omega t}\rightarrow M_\Sigma(\cos\theta)e^{i(\omega t+\varphi_\Sigma)}\hat{\mathbf{z}}+M_\Pi(\sin\theta)e^{i(\omega t+\varphi_\Pi)}\hat{\mathbf{x}} \,, \tag{28}$$

which amounts to considering two oscillating dipoles

$$\tilde{\mathbf{M}}_1=M_\Pi(\sin\theta)\hat{\mathbf{x}}+M_\Sigma(\cos\theta)\cos(\varphi_\Sigma-\varphi_\Pi)\hat{\mathbf{z}}$$

and

$$\tilde{\mathbf{M}}_2=M_\Sigma(\cos\theta)\sin(\varphi_\Sigma-\varphi_\Pi)\hat{\mathbf{z}}$$

dephased by $\pi/2$.

#### 4. Spin coupling

In the case of fine (or hyperfine) structure we assume the splitting to be much smaller than the excess energy and larger than the radiative linewidth. This means that the coupling of the spin to the angular momentum occurs in a time scale much shorter than the fluorescence emission and much longer than the dissociation of the molecule. Under these conditions the excitation matrix $\rho_{jm_jj'm_j'}$, in the atomic basis set $|jm_j\rangle$ is given by

$$\tilde{\rho}_{jm_j,j'm_j'}=\sum_{m_L m_L'}\tilde{\rho}_{m_L,m_L'}(-1)^{2L-2S+m_j+m_j'}\frac{[(2j+1)(2j'+1)]^{1/2}}{(2S+1)}\begin{pmatrix} L & S & j \\ m_L & m_S & -m_j\end{pmatrix}\begin{pmatrix} L & S & j' \\ m_L' & m_S & -m_j'\end{pmatrix} \,, \tag{29}$$

where ( ) are 3-$j$ symbols. It should be noticed that we only need the terms of Eq. (29) with $j=j'$.

The effect of the coupling with the spin on the classical oscillating dipole is to make the dipole precess around the atomic angular momentum **j** vector (see Fig. 3).

### E. Fluorescence emission from the fragment

In the uncoupled atomic basis set $|Lm_L\rangle$ the detection-matrix elements $\mathcal{D}_{Lm_L,Lm_L'}$ are given by[20]

$$\mathcal{D}_{Lm_L,Lm_L'}=(k_f^3\mathcal{R}_f^2e^2/4\pi\Gamma^{(\mathrm{at})})\sum_{q,q'=0,\pm1}(-1)^q(e^*)_{-q}e_{-q'}(2L+1)(2L_f+1)$$
$$\times\begin{pmatrix} L & 1 & L_f \\ 0 & 0 & 0\end{pmatrix}\begin{pmatrix} L_f & 1 & L \\ m_f & q & -m_L\end{pmatrix}\begin{pmatrix} L_f & 1 & L \\ m_f & -q' & -m_L'\end{pmatrix} \,, \tag{30}$$

where $e_q$ ($q=0,\pm1$) are the spherical components of the polarization vector, i.e.,

$$e_0=e_z, \quad e_{\pm1}=\mp\frac{1}{\sqrt{2}}(e_x\pm ie_y) \,, \tag{31}$$

where $x,y,z$ are the Cartesian components in the molecular frame.

In the coupled atomic basis set $|jm_j\rangle$ on the other hand, the detection-matrix elements $\mathcal{D}_{jm_jjm_j'}$ are given by[20]

$$\mathcal{D}_{jm_j,j'm_j'}=\frac{k_f^3\mathcal{R}_f^2e^2}{4\pi\Gamma^{(\mathrm{at})}}\sum_{k,\mu,q,q'}(e^*)_{-q}e_{-q'}(-1)^{S-L_f-j-j'+m_j'}$$

$$\times(2L+1)(2L_f+1)[(2j+1)(2j'+1)]^{1/2}\begin{bmatrix} L & 1 & L_f \\ 0 & 0 & 0 \end{bmatrix}^2$$
$$\times(2k+1)\begin{bmatrix} 1 & 1 & k \\ -q & -q' & \mu \end{bmatrix}\begin{bmatrix} j & j' & k \\ -m_j & m_j' & -\mu \end{bmatrix}\begin{Bmatrix} L & L & k \\ j' & j & S \end{Bmatrix}\begin{Bmatrix} L & L & k \\ 1 & 1 & L_f \end{Bmatrix}, \tag{32}$$

where { } are 6-$j$ symbols.

Equation (32) together with Eq. (29) constitute, when introduced in Eqs. (17) and (18), the general expressions in the axial-recoil approximation leading to the fluorescence cross sections for a given orientation of the molecule specified by the polar angles $\theta$ and $\Phi$. Since usually the molecules are initially randomly oriented an average over $\theta$ and $\Phi$ should be performed.

## III. RESULTS FOR THE CASES WHERE THE INITIAL STATE IS $^1\Sigma$

### A. $AB(^1\Sigma)+h\nu\rightarrow AB^*(^1\Sigma,^1\Pi)\rightarrow A^*(^1P)+B(^1S)$ $\rightarrow A(^1S)+B(^1S)+h\nu'$

From Eqs. (18), (19), and (30), it is obtained

$$d\sigma/d\hat{\Omega}_f=4\pi^2k_i(3Q/8\pi)[2\rho_{1,1}e_x^2+\rho_{0,0}e_z^2 +2\sqrt{2}\rho_{0,1}e_ze_x\cos(\varphi_\Sigma-\varphi_\Pi)], \tag{33}$$

where $Q$ is the branching ratio for the particular transition which is studied and $\varphi_\Sigma$ and $\varphi_\Pi$ the vibrational phases for the two dissociative continua $AB^*(\Sigma,\Pi)$. In Eq. (33) $e_x,e_y,e_z$ denote the components of the polarization vector on the molecular frame. In order to calculate the polarization ratio we need the intensities parallel and perpendicular to the space-fixed $Z$ axis. We then use the transformation

$$\begin{bmatrix}\hat{x}\\ \hat{y}\\ \hat{z}\end{bmatrix}=\begin{bmatrix}\cos\theta\cos\Phi & \cos\theta\sin\Phi & -\sin\theta\\ -\sin\Phi & \cos\Phi & 0\\ \sin\theta\cos\Phi & \sin\theta\sin\Phi & \cos\theta\end{bmatrix}\begin{bmatrix}\hat{X}\\ \hat{Y}\\ \hat{Z}\end{bmatrix} \tag{34}$$

between the space-fixed components $e_Xe_Ye_Z$ and the molecular-frame components $e_xe_ye_z$ with $\theta$ and $\Phi$ being the polar angles specifying the direction of the molecular axis with respect to the space-fixed system. The parallel polarization is then $e_\parallel=e_Z$ defined in our case by the polarization of the incident photon and the perpendicular polarization can be arbitrarily set to $e_\perp=e_X$. We obtain

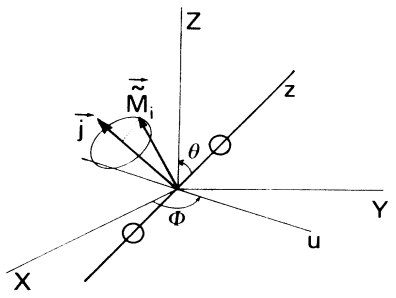


FIG. 3. Precession of the oscillating dipoles $\mathbf{M}_i$ around the atomic angular moment $\mathbf{J}$ induced by the spin-orbit coupling.

$$(d\sigma/d\hat{\Omega}_f)_\parallel=4\pi^2k_i\left[\frac{3Q}{8\pi}\right][(\sin^4\theta)M_\Pi^2+(\cos^4\theta)M_\Sigma^2 +2(\cos^2\theta)(\sin^2\theta)M_\Sigma M_\Pi \times\cos(\varphi_\Sigma-\varphi_\Pi)], \tag{35a}$$

$$(d\sigma/d\hat{\Omega}_f)_\perp=4\pi^2k_i\left[\frac{3Q}{8\pi}\right](\sin^2\theta)(\cos^2\theta)(\cos^2\Phi) \times[M_\Pi^2+M_\Sigma^2-2M_\Sigma M_\Pi\cos(\varphi_\Sigma-\varphi_\Pi)]. \tag{35b}$$

Equations (35) provide the intensities for parallel and perpendicular polarizations when the molecule has a well-defined orientation $\theta,\Phi$. We need now to average Eqs. (35) over $\theta$ and $\Phi$. The final result is

$$\left[\frac{d\sigma}{d\hat{\Omega}_f}\right]_\parallel=4\pi^2k_i\left[\frac{3Q}{8\pi}\right]\frac{1}{15} \times[8M_\Pi^2+3M_\Sigma^2+4M_\Sigma M_\Pi\cos(\varphi_\Sigma-\varphi_\Pi)], \tag{36a}$$

$$\left[\frac{d\sigma}{d\hat{\Omega}_f}\right]_\perp=4\pi^2k_i\left[\frac{3Q}{8\pi}\right]\frac{1}{15} \times[M_\Pi^2+M_\Sigma^2-2M_\Sigma M_\Pi\cos(\varphi_\Sigma-\varphi_\Pi)]. \tag{36b}$$

The sum over all polarizations and all possible directions $\hat{\Omega}_f$ is known to be equal to the sum over each polarization $e_X,e_Y,e_Z$ observed transversally affected by a $8\pi/3$ geometrical factor. Thus

$$\sigma\equiv(8\pi/3)[(d\sigma/d\hat{\Omega}_f)_\parallel+2(d\sigma/d\hat{\Omega}_f)_\perp] =\frac{4\pi^2}{3}k_i(2M_\Pi^2+M_\Sigma^2)Q \tag{37}$$

which is the expected photodissociation cross section multiplied by the branching ratio $Q$ of the observed transition. The polarization ratio will then be

$$P\equiv\frac{(d\sigma/d\hat{\Omega}_f)_\parallel-(d\sigma/d\hat{\Omega}_f)_\perp}{(d\sigma/d\hat{\Omega}_f)_\parallel+(d\sigma/d\hat{\Omega}_f)_\perp} =\frac{7M_\Pi^2+2M_\Sigma^2+6M_\Sigma M_\Pi\cos(\varphi_\Sigma-\varphi_\Pi)}{9M_\Pi^2+4M_\Sigma^2+2M_\Sigma M_\Pi\cos(\varphi_\Sigma-\varphi_\Pi)}. \tag{38}$$

From Eq. (38) it is now easy to obtain

$$P=\tfrac{1}{2}\quad\text{for } M_\Pi=0, \tag{39a}$$

$$P=\tfrac{7}{9} \quad \text{for } M_\Sigma=0 \ , \tag{39b}$$

which are the previously published results for $^1\Sigma\rightarrow{}^1\Sigma$ and $^1\Sigma\rightarrow{}^1\Pi$ transitions,[8] respectively.

### B. $AB(^1\Sigma)+h\nu\rightarrow AB^*(^1\Sigma,{}^1\Pi)\rightarrow A^*(^2P)+B(^2S)\rightarrow A(^2S)+B(^2S)+h\nu'$

From Eqs. (18), (19), and (32), we now have for the two components $j=\frac{1}{2}$ and $j=\frac{3}{2}$

$$(d\sigma/d\hat{\Omega}_f)_{j=1/2}=4\pi^2k_i\left(\frac{3Q}{8\pi}\right)[\rho_{0,0}+2\rho_{1,1}](e_x^2+e_y^2+e_z^2)\tfrac{1}{9} \ , \tag{40a}$$

$$(d\sigma/d\hat{\Omega}_f)_{j=3/2}=4\pi^2k_i\left(\frac{3Q}{8\pi}\right)\left[\rho_{0,0}(1+3e_z^2)\tfrac{1}{9}+\tfrac{2}{9}\rho_{1,1}(1+3e_x^2)+\frac{4}{3\sqrt{2}}\rho_{1,0}e_xe_z\cos(\varphi_\Sigma-\varphi_\Pi)\right] . \tag{40b}$$

Since $e_x^2+e_y^2+e_z^2=1$, it is clear from Eq. (40a) that the emission from the $j=\frac{1}{2}$ level is isotropic as expected for an incident linear polarization which can only produce alignment and not optical orientation.

Performing as in Sec. III A the average over all possible orientations of the molecule we obtain

$$(d\sigma/d\hat{\Omega}_f)_{\parallel j=1/2}=(d\sigma/d\hat{\Omega}_f)_{\perp j=\frac{1}{2}}=\frac{4\pi^2}{3}k_i\left(\frac{3Q}{8\pi}\right)(\tfrac{2}{9}M_\Pi^2+\tfrac{1}{9}M_\Sigma^2) \ , \tag{41a}$$

$$(d\sigma/d\hat{\Omega}_f)_{\parallel j=\frac{3}{2}}=\frac{4\pi^2}{3}k_i\left(\frac{3Q}{8\pi}\right)\times[\tfrac{14}{45}M_\Sigma^2+\tfrac{34}{45}M_\Pi^2+\tfrac{4}{15}M_\Sigma M_\Pi\cos(\varphi_\Sigma-\varphi_\Pi)] \ , \tag{41b}$$

$$(d\sigma/d\hat{\Omega}_f)_{\perp j=\frac{3}{2}}=\frac{4\pi^2}{3}k_i\left(\frac{3Q}{8\pi}\right)\times[\tfrac{8}{45}M_\Sigma^2+\tfrac{13}{45}M_\Pi^2-\tfrac{2}{15}M_\Sigma M_\Pi\cos(\varphi_\Sigma-\varphi_\Pi)] \ . \tag{41c}$$

If the emissions from $j=\frac{1}{2}$ and $j=\frac{3}{2}$ are resolved, the polarization ratio is $P_{1/2}=0$ for the $j=\frac{1}{2}$ emission and

$$P_{3/2}=\frac{6M_\Sigma^2+21M_\Pi^2+18M_\Sigma M_\Pi\cos(\varphi_\Sigma-\varphi_\Pi)}{22M_\Sigma^2+47M_\Pi^2+6M_\Sigma M_\Pi\cos(\varphi_\Sigma-\varphi_\Pi)} \tag{42}$$

for the $j=\frac{3}{2}$ emission. From Eq. (42) one obtains

$$P=\tfrac{3}{11} \quad \text{for } M_\Pi=0 \ , \tag{43a}$$

$$P=\tfrac{21}{47} \quad \text{for } M_\Sigma=0 \ , \tag{43b}$$

which have been given by Singer *et al.*[10]

Equations (43) as compared with Eq. (39) demonstrate the effect of depolarization due to fine structure.

If on the contrary the two fine- (or hyperfine-) structure components are unresolved, we get

$$P=\frac{6M_\Sigma^2+21M_\Pi^2+18M_\Sigma M_\Pi\cos(\varphi_\Sigma-\varphi_\Pi)}{32M_\Sigma^2+67M_\Pi^2+6M_\Sigma M_\Pi\cos(\varphi_\Sigma-\varphi_\Pi)} \tag{44}$$

which for the limiting cases $M_\Sigma=0$ or $M_\Pi=0$ provides the new results

$$P=\tfrac{3}{16} \quad \text{for } M_\Pi=0 \ , \tag{45a}$$

$$P=\tfrac{21}{67} \quad \text{for } M_\Sigma=0 \ , \tag{45b}$$

which are lower than those obtained in the fine-structure resolved case [see Eq. (43)], as expected since the $j=\frac{1}{2}$ component is unpolarized. We should also notice from Eqs. (45) and (39) the somewhat striking result that the polarization of the fluorescence is drastically reduced even if all the components of the fine (or hyperfine) structure are simultaneously detected.

It is also useful to note that Eq. (44) can be obtained directly from the individual polarization $P_{3/2}$ given in Eq. (42) using the statistical weight of the two components $j=\frac{1}{2}$ and $j=\frac{3}{2}$.

### C. Other cases involving a $A^*(D)$ fragment

In this section we consider two cases where the excited atomic fragment is in a singlet or a doublet $D$ state. We there have from an initial $^1\Sigma$ state

$$AB(^1\Sigma)+h\nu\rightarrow AB^*(^1\Sigma,{}^1\Pi)\rightarrow A^*(^{1,2}D)+B(^{1/2}S)\rightarrow A(^{1,2}P)+B(^{1,2}S)=h\nu' \ .$$

The results for these two cases are summarized in Tables I and II.

## IV. INTERPRETATION AND DISCUSSION

In Sec. III we have applied the general formalism to photodissociation processes involving the coherent excitation of $^1\Sigma$ and $^1\Pi$ dissociative states. In particular, for the case

$$AB(^1\Sigma)+h\nu\rightarrow AB^*(^1\Sigma,{}^1\Pi)\rightarrow A^*(^1P)+B(^1S)\rightarrow A(^1S)+B(^1S)+h\nu' \ ,$$

we have obtained the polarization rate given in Eq. (38), where $M_\Sigma$ and $M_\Pi$ are the transition dipole-moment amplitudes for excitation of the $^1\Sigma$ and $^1\Pi$ dissociative states, while $\varphi_\Sigma$ and $\varphi_\Pi$ are the quantum-mechanical dephasings accumulated during the dissociation.

### A. Interpretation in terms of classical oscillating dipoles

It is possible to obtain the polarization ratio Eq. (38) using the classical model of the oscillating dipole. The

TABLE I. Parallel and perpendicular fluorescence cross sections for the $^1D \rightarrow {}^1P$ and $^2D \rightarrow {}^2P$ fragment transitions in units of $4\pi^2 k_i (3Q/8\pi)$.

| | $\sigma_\parallel$ | $\sigma_\perp$ |
|---|---|---|
| $^1D \rightarrow {}^1P$ | $\frac{7}{15}M_\Sigma^2 + M_\Pi^2 + \frac{2}{5\sqrt{3}}M_\Sigma M_\Pi \cos(\varphi_\Sigma - \varphi_\Pi)$ | $\frac{4}{15}M_\Sigma^2 + \frac{1}{2}M_\Pi^2 - \frac{1}{5\sqrt{3}}M_\Sigma M_\Pi \cos(\varphi_\Sigma - \varphi_\Pi)$ |
| $^2D_{5/2} \rightarrow {}^2P_{3/2}$ | $\frac{33}{125}M_\Sigma^2 + \frac{14}{25}M_\Pi^2 - \frac{8\sqrt{3}}{125}M_\Sigma M_\Pi \cos(\varphi_\Sigma - \varphi_\Pi)$ | $\frac{21}{125}M_\Sigma^2 + \frac{8}{25}M_\Pi^2 + \frac{4\sqrt{3}}{125}M_\Sigma M_\Pi \cos(\varphi_\Sigma - \varphi_\Pi)$ |
| $^2D_{3/2} \rightarrow {}^2P_{3/2,1/2}$ | $\frac{64}{375}M_\Sigma^2 + \frac{9}{25}M_\Pi^2 - \frac{14\sqrt{3}}{375}M_\Sigma M_\Pi \cos(\varphi_\Sigma - \varphi_\Pi)$ | $\frac{43}{375}M_\Sigma^2 + \frac{11}{50}M_\Pi^2 + \frac{7\sqrt{3}}{375}M_\Sigma M_\Pi \cos(\varphi_\Sigma - \varphi_\Pi)$ |
| $^2D_{3/2,5/2} \rightarrow {}^2P_{3/2,1/2}$ | $\frac{163}{375}M_\Sigma^2 + \frac{23}{25}M_\Pi^2 - \frac{38\sqrt{3}}{375}M_\Sigma M_\Pi \cos(\varphi_\Sigma - \varphi_\Pi)$ | $\frac{106}{375}M_\Sigma^2 + \frac{27}{50}M_\Pi^2 + \frac{19\sqrt{3}}{375}M_\Sigma M_\Pi \cos(\varphi_\Sigma - \varphi_\Pi)$ |

electric dipole induced by the photon absorption $\mathbf{M}$, as given in Eq. (23), has components along both the molecular $\hat{\mathbf{z}}$ and $\hat{\mathbf{x}}$ axes. These components are dephased during dissociation according to Eq. (28) in the axial-recoil approximation, i.e., if the molecule does not rotate while dissociating. The fluorescence emission can be interpreted as the emission of these $\tilde{\mathbf{M}}$ oscillating dipoles. The actual calculation proceeds as follows. Since the parallel and perpendicular fluorescence intensities refer to the laboratory frame, $\tilde{\mathbf{M}}$ has to be given in that reference system. Using Eq. (34) into Eq. (28) we obtain

$$\tilde{\mathbf{M}}_1 = [M_\pi - M_\Sigma \cos(\varphi_\Sigma - \varphi_\Pi)](\sin\theta)(\cos\theta) \times [(\cos\Phi)\hat{\mathbf{X}} + (\sin\Phi)\hat{\mathbf{Y}}] + [M_\Pi \sin^2\theta + M_\Sigma(\cos^2\theta)\cos(\varphi_\Sigma - \varphi_\Pi)]\hat{\mathbf{Z}} \tag{46a}$$

and

$$\tilde{\mathbf{M}}_2 = -\sin(\varphi_\Sigma - \varphi_\Pi)M_\Sigma(\sin\theta)(\cos\theta) \times [(\cos\Phi)\hat{\mathbf{X}} + (\sin\Phi)\hat{\mathbf{Y}}] \tag{46b}$$

from which we obtain

$$I_\parallel \propto \langle (\tilde{\mathbf{M}}_1 \cdot \hat{\mathbf{Z}})^2 + (\tilde{\mathbf{M}}_2 \cdot \hat{\mathbf{Z}})^2 \rangle = \langle M_\Pi^2 \sin^4\theta + M_\Sigma^2 \cos^4\theta + 2M_\Pi M_\Sigma (\sin^2\theta)(\cos^2\theta)\cos(\varphi_\Sigma - \varphi_\Pi) \rangle$$
$$= \frac{1}{15}[8M_\Pi^2 + 3M_\Sigma^2 + 4M_\Sigma M_\Pi \cos(\varphi_\Sigma - \varphi_\Pi)] \tag{47}$$

and

$$I_\perp \propto \langle (\tilde{\mathbf{M}}_1 \cdot \hat{\mathbf{X}})^2 + (\tilde{\mathbf{M}}_2 \cdot \hat{\mathbf{X}})^2 \rangle = \langle [M_\Pi^2 + M_\Sigma^2 - 2M_\Pi M_\Sigma \cos(\varphi_\Sigma - \varphi_\Pi)](\sin^2\theta)(\cos^2\theta)(\cos^2\Phi) \rangle$$
$$= \frac{1}{15}[M_\Pi^2 + M_\Sigma^2 - 2M_\Pi M_\Sigma \cos(\varphi_\Sigma - \varphi_\Pi)] \, . \tag{48}$$

It is now straightforward to obtain Eq. (38) from Eqs. (47) and (48). It is clear from Eqs. (46) that the cross term in Eqs. (47) and (48) involving the phase difference $(\varphi_\Sigma - \varphi_\Pi)$ arises from $\tilde{\mathbf{M}}_1$, the oscillating dipole which components along $\hat{\mathbf{x}}$ and $\hat{\mathbf{z}}$ remain in phase i.e., the remaining coherence of the initial dipole.

We shall consider now some particular cases. When $M_\Pi = 0$, i.e., for a pure parallel $\Sigma \rightarrow \Sigma$ transition, the oscillating dipole is created along $\hat{\mathbf{z}}$ where it remains during the dissociation. Since the excitation probability is proportional to $\cos^2\theta$ there is a preferential angular distribution of the excited molecules and hence of the excit-

TABLE II. Polarization ratios for the $^1D \rightarrow {}^1P$ and $^2D \rightarrow {}^2P$ fragment fluorescence. $P_\Pi$ and $P_\Sigma$ are the values obtained for excitation of pure $\Pi$ and $\Sigma$ states, respectively.

| | $P$ | $P_\Pi$ | $P_\Sigma$ |
|---|---|---|---|
| $^1D \rightarrow {}^1P$ | $\frac{6M_\Sigma^2 + 15M_\Pi^2 + 6\sqrt{3}M_\Sigma M_\pi \cos(\varphi_\Sigma - \varphi_\Pi)}{22M_\Sigma^2 + 45M_\Pi^2 + 2\sqrt{3}M_\Sigma M_\Pi \cos(\varphi_\Sigma - \varphi_\Pi)}$ | $\frac{1}{3} \cong 0.33$ | $\frac{3}{11} \cong 0.27$ |
| $^2D_{5/2} \rightarrow {}^2P_{3/2}$ | $\frac{12M_\Sigma^2 + 30M_\Pi^2 - 12\sqrt{3}M_\Sigma M_\Pi \cos(\varphi_\Sigma - \varphi_\Pi)}{63M_\Sigma^2 + 110M_\Pi^2 - 4\sqrt{3}M_\Sigma M_\Pi \cos(\varphi_\Sigma - \varphi_\Pi)}$ | $\frac{3}{11} \cong 0.27$ | $\frac{4}{21} \cong 0.19$ |
| $^2D_{3/2} \rightarrow {}^2P_{3/2,1/2}$ | $\frac{42M_\Sigma^2 + 105M_\Pi^2 - 42\sqrt{3}M_\Sigma M_\Pi \cos(\varphi_\Sigma - \varphi_\Pi)}{214M_\Sigma^2 + 435M_\Pi^2 - 14\sqrt{3}M_\Sigma M_\Pi \cos(\varphi_\Sigma - \varphi_\Pi)}$ | $\frac{7}{29} \cong 0.24$ | $\frac{21}{107} \cong 0.20$ |
| $^2D_{5/2,3/2} \rightarrow {}^2P_{3/2,1/2}$ | $\frac{114M_\Sigma^2 + 285M_\Pi^2 - 114\sqrt{3}M_\Sigma M_\Pi \cos(\varphi_\Sigma - \varphi_\Pi)}{592M_\Sigma^2 + 1095M_\Pi^2 - 38\sqrt{3}M_\Sigma M_\Pi \cos(\varphi_\Sigma - \varphi_\Pi)}$ | $\frac{19}{73} \cong 0.26$ | $\frac{57}{296} \cong 0.19$ |

ed fragments along the $\hat{\mathbf{Z}}$ laboratory axis. The oscillating dipole has components $\cos\theta$ and $\sin\theta\cos\Phi$ along the $\hat{\mathbf{Z}}$ and $\hat{\mathbf{X}}$ axes, respectively. Therefore for a given orientation of the molecule,

$$I_{\parallel} \propto \cos^4\theta, \quad I_{\perp} \propto \cos^2\theta \sin^2\theta \cos^2\Phi ,$$

and after averaging over all possible orientations one obtains the well-known result that the polarization ratio is $P=\frac{1}{2}$. This case is the only one where usual classical formula [Eq. (2)] is valid with $\gamma=0$.

When $M_{\Sigma}=0$, i.e., for a pure perpendicular $\Sigma\rightarrow\Pi$ transition, the oscillating dipole is created along $\hat{\mathbf{x}}$ where it remains if dissociation is fast, with a probability $\sin^2\theta$. The emitting dipole must be along $\hat{\mathbf{x}}$ too and has components $-\sin\theta$ and $\cos\theta\cos\Phi$ along the $\hat{\mathbf{Z}}$ and $\hat{\mathbf{X}}$ laboratory axes, respectively. The polarization ratio obtained after averaging over all possible initial orientations of the internuclear axis is then $P=\frac{7}{9}$. We notice that this value obtained quantum mechanically[8,9] is actually a classical result. It is obvious that Eq. (2) cannot apply to this case since the maximum possible value of $P$ using this equation is $\frac{1}{2}$. The reason for the failure of the usual classical formula (2) is an abusive average over the orientation of the initial dipole around the internuclear axis. In a correct classical treatment one should realize that the initial oscillating dipole must lie in the plane $\hat{\mathbf{z}}\hat{\mathbf{Z}}$, which corresponds in quantum mechanics to a coherent superposition of $\Lambda=\pm1$ states.[8,9]

When the dephasing $\varphi_{\Sigma}-\varphi_{\Pi}$ is equal to $\pm\pi/2$ the polarization ratio reduces to the result of a simple incoherent superposition of $\Sigma\rightarrow\Sigma$ and $\Sigma\rightarrow\Pi$ photodissociation processes. In that case the two components $\tilde{M}_x$ and $\tilde{M}_z$ (see Fig. 2) are oscillating in quadrature and they add their intensities.

An interesting particular case is obtained for $M_{\Pi}=M_{\Sigma}$ and $\varphi_{\Sigma}-\varphi_{\Pi}=0$. We have already noted (see Sec. II D 2) that this corresponds to an isotropic angular distribution of the fragments. From Eq. (38) we have $P=1$ for this case. This provides a particularly striking example of a maximum of the polarization of the photofragment fluorescence associated with a fully isotropic fragment distribution. The particular case considered here is very unrealistic. It corresponds to the atomic case where the induced oscillating dipole is along the $\hat{\mathbf{Z}}$ axis (see Fig. 2). The emitting dipole being along the laboratory $\hat{\mathbf{Z}}$ axis the polarization of the fluorescence is fully parallel to the incident polarization ($P=1$).

### B. Discussion of the results for the case

$$AB(^1\Sigma)+h\nu \rightarrow AB^*(^1\Sigma,{}^1\Pi) \rightarrow A^*(^1P)+B(^1S) \rightarrow A(^1S)+B(^1S)+h\nu'$$

Equation (38) gives the polarization ratio $P$ for the case of an initial $^1\Sigma$ state which after photon absorption dissociates into $A^*(^1P)+B(^1S)$ fragments. The polarization ratio depends on the relative excitation amplitude $\chi=M_{\Sigma}/M_{\Pi}$ of the two possible excited-dissociative paths, and on the dephasing $\Delta\varphi=\varphi_{\Sigma}-\varphi_{\Pi}$ of the vibrational wave functions in these two states. In Fig. 4 we present the limiting values of $P$ ($P_+$ corresponding to $\Delta\varphi=0$ and $P_-$ to $\Delta\varphi=\pi$) as a function of $\chi$. The possible values of $P$ lie necessarily between these two curves. It is seen that $P_{\pm}$ changes rapidly around $\chi=0$ which implies that a small contribution of the $\Sigma$ state to the photodissociation through the $\Pi$ state can change appreciably the polarization ratio. Complementarily the slow approach to the asymptote at large $\chi$ means that the reverse is also true, a small contribution of the $\Pi$ state to a $\Sigma$-state photodissociation process can induce a large change on $P$.

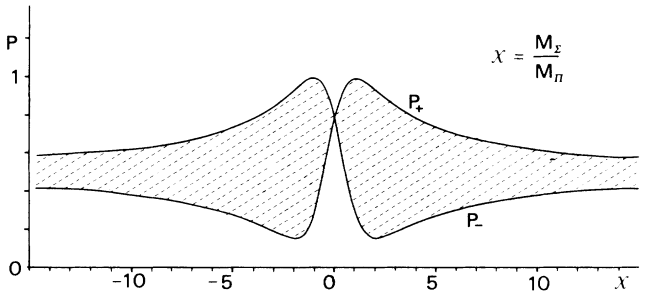


FIG. 4. Maximum $P_+$ and minimum $P_-$ possible values of the polarization ratio (see text) as a function of the relative excitation amplitude $\chi$. The possible values of $P$ lie necessarily in the shaded area and depend on the relative phases of the vibrational wave functions at large internuclear distances.

In Fig. 5 we present a study of the possible relation between the polarization ratio $P$ and the angular distribution parameter $\beta$ [see Eq. (27)]. Since $\beta$ depends only on $\chi^2$ while $P$ depends both on $\chi$ and $\Delta\varphi$, for a given value of $\beta$, $P$ can have a whole range of values between $P_+$ and $P_-$. This defines the shaded region in Fig. 5.

### C. Application to $Ca_2$ photodissociation

The preceding study provides a possible explanation of the observed polarization ratio in the case of photodissociation of $Ca_2$. For excitation at $\lambda=406$ nm Vigué *et al.*[8] measured $P=0.64\pm0.01$.

The interpretation of this very large polarization ratio was provided in terms of the single process

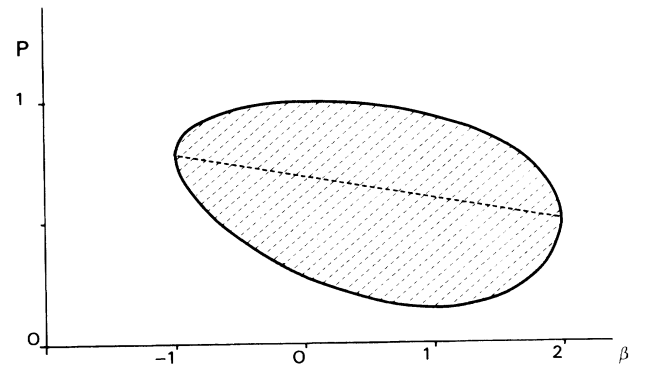


FIG. 5. Parametric dependence of the polarization ratio $P$ vs the anisotropy parameter $\beta$ of the angular distribution of the fragments. The solid curve represents $P_+$ and $P_-$ superposed. The heavy dashed curve represents the results for $\Delta\varphi=\pi/2$ (see text).

$$Ca_2(^1\Sigma)+h\nu\rightarrow Ca_2(^1\Pi)\rightarrow Ca(^1P)+Ca(^1S)\ ,$$

for which the value $P=\frac{7}{9}=0.78$ is expected[8,9] [see Eq. (39)]. The difference between the theoretical and the experimental values was attributed to saturation and fluorescence-trapping effects. An alternative explanation can be provided by our study. If the relative population $\sigma_\Sigma/\sigma_\Pi=\chi^2/2$ of the $\Sigma$ and $\Pi$ states is as little as 3.5% ($\chi=0.26$) then assuming $(\varphi_\Sigma-\varphi_\Pi)=\pi$, we obtain from Eq. (38) $P\cong 0.64$. In addition, the value of $P$ observed for excitations at $\lambda=413$ nm, $P=0.68$, can be explained with the same value for $\chi$ and a phase difference $(\varphi_\Sigma-\varphi_\Pi)\sim\pm\pi/4$, which is a reasonable variation according to our numerical calculation on a similar case.[23] Actually, this interference effect between $\Pi$ and $\Sigma$ dissociative states was suggested already in Ref. 9. The above calculation shows that even a weak excitation of the $\Sigma$ continuum can significantly modify the polarization ratio.

### D. Discussion of the results for other cases

We have discussed the results obtained in Sec. III A for the singlet $P$-excited atomic fragment. In Sec. III B we have considered the case where the excited fragment is in a $^2P$ state. The results both for resolved or unresolved fine-structure fluorescence components show that the spin coupling induces a substantial depolarization and washes out partially the interference effects. This is the result, as discussed in Sec. II D, of the precession of the oscillating dipole around the direction of the atomic electronic angular momentum **J**.

In Fig. 6 we present the limiting values of $P$ as a function of $\chi$ for this case. Comparison with Fig. 5 shows clearly the depolarization effect of the spin coupling, the maximum of $P=1$ in the singlet case is now reduced to $P=0.43$.

For the cases discussed in Sec. III C which involve a simplet or a doublet $D$-state excited fragment, the classical picture does not keep the simple form presented above for the $P\rightarrow S$ case. The identification of the emitting dipoles with the $\tilde{M}_i$ dipoles (see Sec. II D 3) created by the photodissociation does not hold anymore.

In any case, the final result cannot be but a lesser polarization ratio. From Table I we deduce that the extrema of the polarization ratio are $0.45\geq P\geq 0.17$ for a $^1D$ and $0.36\geq P\geq 0.037$ for a $^2D$.

## V. CONCLUSIONS

In this paper we have presented a quite general treatment of the coherence effects in the polarization of the light emitted by atomic photofragments in the case where fluorescence occurring at short internuclear distances is negligible, i.e., when the fluorescence lifetime is much longer than the dissociation time. One such coherence effect is the previously studied[8,9] interference between the emission from the $m_L=\pm\Lambda$ components issued from the dissociation of a single $\Lambda$ molecular state. In addition, we have shown that the coherent excitation of the manifold of electronic molecular states dissociating to the same atomic state induces a new interference effect in the fluorescence polarization. As opposed to the former the latter depends on the ratio of the photoabsorption amplitudes for excitation of the different electronic states as well as on the relative phases of the corresponding vibrational dissociative wave functions at large internuclear distances.

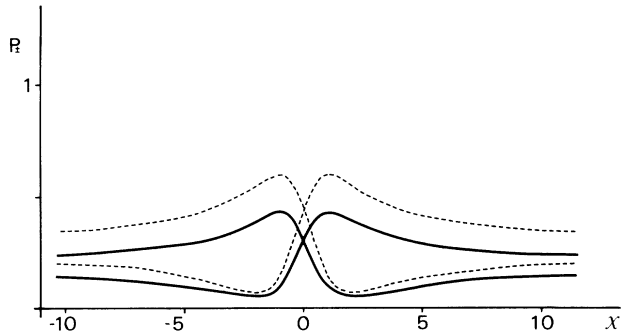


FIG. 6. Same as Fig. 4 for the spin-doublet case. The dashed curves represent the limiting values $P_\pm$ of the polarization ratio for the $j=\frac{3}{2}$ resolved component. The solid lines correspond to the unresolved case (see text).

In general the photoabsorption amplitude ratios are smooth functions of the excess energy. On the contrary, the phase difference is more likely to vary rapidly with the excess energy.[22] We have shown that the interference effect introduces a term in the expression for the fluorescence intensities that depends on the cosine of the phase difference. Therefore, we predict an oscillating behavior of the fluorescence polarization ratio as a function of the photon energy.

We have considered different particular cases corresponding to a diatomic molecule initially in a $^1\Sigma$ state. We have shown that a small mixture of $^1\Sigma$ and $^1\Pi$ excited continua may lead to a sensible change of the polarization ratio. This effect may provide a possible explanation for the observed polarization ratio of the fluorescence from the Ca* fragments in the photodissociation of $Ca_2$.[8]

We have studied the depolarization effect induced by the spin-orbit coupling for the case where the dissociation occurs in a time scale much shorter than the spin coupling. We have shown that this operates even in the case where the fine-structure components are unresolved. This is also valid for the case of hyperfine structure if the splitting is larger than the natural width.

Finally it is worth noting that the coherent effects discussed in this work are not pure quantum effects as they can be interpreted within a classical oscillating dipole model if the averages over initial orientations are properly performed.

## ACKNOWLEDGMENT

The Laboratoire de Spectroscopic Hertzienne de l'Ecole Normale Supérieure is "Laboratoire associé au centre National de la Recherche Scientifique (CNRS)." The Laboratoire pour l'Utilisation du Rayonnement Electromagnétique is "Laboratoire du CNRS, Commisariat à l'Energie Atomique, et Ministère de l'Education Nationale."

[1]R. J. van Brunt and R. N. Zare, J. Chem. Phys. **48**, 4304 (1968).
[2]G. A. Chamberlain and J. P. Simons, Chem. Phys. Lett. **32**, 355 (1975); J. Chem. Soc. Faraday II **71**, 2043 (1975).
[3]M. J. MacPherson, J. P. Simons, and R. N. Zare, Mol. Phys. **38**, 2049 (1979).
[4]J. Husain, J. R. Wiesenfeld, and R. N. Zare, J. Chem. Phys. **72**, 2479 (1980).
[5]E. W. Rothe, U. Krause, and R. Duren, Chem. Phys. Lett. **72**, 100 (1980).
[6]G. W. Loge and R. N. Zare, Mol. Phys. **43**, 1419 (1981).
[7]G. W. Loge and J. R. Wiesenfeld, Chem. Phys. Lett. **78**, 32 (1981).
[8]J. Vigué, P. Grangier, G. Roger, and A. Aspect, J. Phys. (Paris), Lett. **42**, L-531 (1981).
[9]J. Vigué, J. A. Beswick, and M. Broyer, J. Phys. (Paris), Colloq. **44**, 1225 (1983).
[10]S. J. Singer, K. F. Freed, and Y. B. Band, J. Chem. Phys. **79**, 6060 (1983).
[11]H. Hemmati, W. M. Fairbank, Jr., P. K. Boyer, and G. J. Collins, Phys. Rev. A **28**, 567 (1983).
[12]J. Vigué, P. Grangier, and A. Aspect, Phys. Rev. A **30**, 3317 (1984).
[13]B. I. Stepanov and V. P. Gribkovskii, *Theory of Luminescence,* (Ilife Books, London, 1968).
[14]G. J. Diebold, Phys. Rev. Lett. **51**, 1344 (1983).
[15]Ph. Grangier, A. Aspect, and J. Vigué, Phys. Rev. Lett. **54**, 418 (1985).
[16]G. J. Diebold, Phys. Rev. A **32**, 1458 (1985).
[17]G. Kurizki and A. Ben-Reuven, Phys. Rev. A **32**, 2560 (1985).
[18]H. A. Bethe and E. E. Salpeter, *Quantum Mechanics of One- and Two-electron Atoms* (Springer-Verlag, Berlin, 1957).
[19]E. A. Gordeev, E. E. Nikitin, and A. I. Shushin, Mol. Phys. **33**, 1611 (1977).
[20]C. Cohen-Tannoudji, Ann. Phys. (Paris) **7**, 423 (1962).
[21]J. T. Houguen, *The Calculation of Rotational Energy Levels and Rotational Line Intensities in Diatomic Molecules,* Natl. Bur. Stand. (U.S.) Monograph Publ. No. 115 (U.S. GPO, Washington, D.C., 1970).
[22]R. N. Zare, Mol. Photochem. **4**, 1 (1972).
[23]J. Alberto Beswick and M. Glass-Maujean, Phys. Rev. A **35**, 3339 (1987).